First principles studies of an Si tip on an Si(100)2 × 1 reconstructed surface

First principles studies of an Si tip on an Si(100)2 × 1 reconstructed surface

Dung Q Ly, Leonid Paramonov and Charalampos Makatsoris

School of Engineering and Design, Brunel University, Uxbridge, London UB8 3HP, UK

E-mail: harris.makatsoris@brunel.ac.uk

Abstract
We present a systematic study of the interaction between a silicon tip and a reconstructed
Si(100) 2 × 1 surface by means of total energy calculations using density functional theory. We
perform geometry optimization to obtain the reconstructed Si surface using the local density
approximation and the generalized gradient approximation methods and compare our results
with those obtained experimentally. We then study the effects of the tip of a scanning probe of
an atomic force microscope (AFM) on the behaviour of atoms on the reconstructed surface
when the tip translates at distances close to it. Our results show that at certain positions of the
tip relative to the surface and depending on the direction of the scan, the Si dimer on the surface
flips, resulting in a local reconstruction of the surface into p(2 × 2) or c(4 × 2) configurations.
These configurations exhibit energies lower by 0.05 eV/dimer than the Si(100)2 × 1 structure.

(Some figures in this article are in colour only in the electronic version)

1. Introduction

In 1986, Binnig *et al* invented the atomic force microscope
(AFM), a new type of microscope that is used to image surfaces
for both conductors and insulators [1] with atomic resolution.
The main principle of operation of this instrument is the
measurement of the forces between the sample surface and
the scanning probe. The AFM can operate in several modes
including the contact mode and the non-contact mode.

Pioneering research with AFM for investigating surface
structures includes that by Giessibl [2], Kitamura and
Iwatsuki [3], and Ueyama *et al* [4]. For the first time,
they showed that, in ultra-high vacuum using the non-contact
AFM mode and operating in the attractive regime on reactive
surfaces they could produce true atomic resolution images of
the surfaces they studied. Since then many authors have carried
out investigations of surface scanning probe interactions both
experimentally [5–24] and theoretically [5, 25–27, 29, 30] on
different kinds of surface. In particular, experimental and
theoretical work on reactive semiconductor surfaces include
Si(111)7 × 7 [6–8, 11], Si(100)2 × 1 [15–17], InP(110) [18],
InAs(110) [19]; on metallic surfaces include Ag(111) [20],
Cu(111) and Cu(100) [21]; and on insulator surfaces include
NaCl(100) [22], α-Al$_2$O$_3$ (0001) [23], KCl(100) [24]. The
conclusion of these works is that short-range chemical
interactions, within the order of a few angstrom, between the

dangling bond of the surface adatom and the dangling bond of
the tip apex account for the quality of the images in non-contact
AFM. This was also pointed out by Pérez *et al* [26, 27] who
used an Si tip over a reactive reconstructed Si(111) surface. In
their system they calculated the total energy, normal force and
force gradient as a function of distance between the tip and the
surface. They showed that only the short-range interaction at
near contact distances (∼2.5–4 Å) is able to provide a variation
in the force gradient across the surface and is strong enough
to achieve atomic resolution. At larger distances (∼5 Å) the
covalent chemical interaction is comparable in magnitude to
the van der Waals (VdW) interaction between the tip and the
surface. However, the covalent chemical interaction dominates
the force gradients probed in non-contact mode AFM.

The correlation between image contrast, force interac-
tions, and distance between tip and surface in non-contact
mode AFM within ultra-high vacuum (UHV) were investigated
experimentally by Uchihashi *et al* [7] for an Si(111)7 × 7 sur-
face. In this experiment they observed that the variation of
VdW or electrostatic interactions contributed to low contrast
images while the chemical interactions were responsible for
high contrast images. They concluded that image contrast cor-
relates to the characteristics of the force gradient. In particular
the discontinuity they obtained in the force gradient versus tip–
surface distance curve is due to the crossover from physical to
chemical bonding interactions between the AFM tip and the Si

adatoms of the surface and it is at such points where a high or low contrast image can be obtained.

In the present work, we employ pseudopotentials within density functional theory (DFT) to carry out a systematic investigation of an Si tip operating in the attractive region over a reactive reconstructed Si(100)2 × 1 surface. The choice of the particular system is motivated by the use of this type of surface not only in semiconductor device fabrication [31] but also in a number of molecular manipulation experiments using scanning probes [32, 33]. The aim of this investigation is thus to elucidate a theoretical understanding of this system using a first principles approach to aid not only in AFM image interpretation but also in designing molecular manipulation and synthesis experiments using scanning probes on the Si(100)2 × 1 surface. One could then use the tip–surface interaction model obtained by our calculations and design experiments which could, for example, include ones similar to those reported recently by Sugimoto *et al* [12–14] performed on different types of surfaces.

In this study we have calculated and presented the total energy, normal force and force gradient as functions of tip–surface distance when the tip scans across the surface in different directions. We have performed these calculations for different attractive regimes including distances between the tip and the surface where virtually no interaction takes place and also at close distances where there is a strong interaction. For these attractive regimes, we performed calculations for both the unconstrained and the constrained system and compared them. For the unconstrained case all atoms in the system are allowed to relax, for the constrained case all atoms are kept fixed during the calculations. By comparing these two cases we demonstrate the large movements of surface atoms under the effect of the tip, especially at the strong attractive regime regions.

To study the tip–surface interactions we first obtained the reconstructed Si(100)2 × 1 surface which we subsequently used in the study. To validate our model of the Si(100)2 × 1 surface we compare the results of our calculations with simulation results from the literature. Also we compare our results with experimental measurements obtained with various methods including both atomic force microscopy (AFM) and scanning tunnelling microscopy (STM) and other experimental methods. Then we present our modelling approach and the results obtained for the tip–surface interaction and provide the theoretical explanation of results obtained with experimental methods. At present, to the best of our knowledge, an investigation of this type involving the particular system is lacking in the scientific literature and we thus aim at filling this gap.

2. Description of the computational model

The system we are considering is a supercell that contains an Si(100)2 × 1 slab and an Si tip. The slab is composed of a number of layers of Si atoms with its atoms on the bottom layer saturated with hydrogen atoms. Atoms on the bottom layer of the slab and the H atoms are always kept fixed during the calculation. The slab is chosen to be thick enough so that
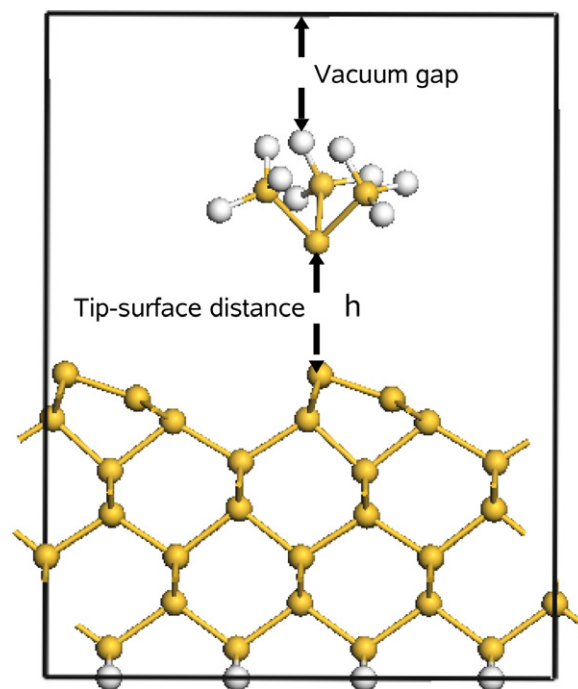

Figure 1. Side view of a supercell containing tip, slab and vacuum gap. A ball-and-stick model of our system with H atoms represented by the brighter coloured balls.

only atoms on the top layers can reconstruct and atoms on the lower layers remain at their bulk positions. We determined the number of layers of the slab by testing convergence of total energy as a function of that number. Following these tests, the number of layers at which the total energy converged at a reasonable computational time was determined at seven layers.

The tip was modelled as a single crystal Si comprising of four Si atoms. The Si atoms at the base of the tip are saturated with H atoms and are kept fixed during calculations. Therefore there is a single dangling bond pointing downwards from the tip apex atom, towards the surface. A similar tip was also used in the work by Pérez *et al* [26–28]. In their work they also studied a larger tip comprised of ten Si atoms [27]. Results of total energy and normal forces obtained for these two different structures were almost identical, suggesting that the short-range tip–surface interaction is dominated by the interaction of the dangling bond of the apex atom with the surface [27]. In both of these models they assumed a single apex atom with a single dangling bond. Here we make the same assumption and employ only the four-Si-atom single crystal tip model. Since we only consider tip–surface interaction and want to completely avoid interaction between the tip and the bottom layers, in the supercell there is a vacuum gap between the tip and the bottom layer of the next supercell that is thick enough to avoid this interaction happening. Using a vacuum gap of 8 Å will satisfy that requirement. The tip and surface structures are shown in figure 1.

The total energy and atomic force are calculated with density functional theory [34], which is implemented in the CASTEP code [35]. For the exchange–correlation term, both the local density approximation (LDA) [36] and generalized

Table 1. Dimer bond length and buckling angle for a reconstructed Si(100)2 × 1 surface obtained from simulations and experiments.

	Method	Dimer bond length (Å)	Buckling angle (deg)	Ref.
First principles calculations	LDA	2.267	18.331	This work
	LDA	2.250	19.000	[39]
	LDA	2.260	18.300	[40]
	GGA	2.304	18.973	This work
	GGA	2.300	15.122	[38]
Experimental measurements	LEED	2.240	19.200	[42]
	X-ray diffraction	2.316	7.400	[41]
	AFM	3.200	—	[16]

gradient approximation (GGA) [37] are used. Ultrasoft pseudopotentials are used for the electron–ion interaction. A plane-wave basis set for the electron wavefunction with a cut-off energy of 450 eV is used. Integrations in the Brillouin zone are performed using special k-points generated with a $2 \times 3 \times 1$ Monkhurst–Pack grid.

Two modes of interaction between the tip and the surface have been investigated. The first mode is concerned with calculations as the tip height varies above a certain position of the surface. The second mode involves calculations at a constant height of the tip above the surface but for different positions across the surface. For each mode, energies and normal forces are determined in a stepwise, quasistatic manner by making small movements of the tip either normal or parallel to the surface. This assumption takes advantage of the fact that the frequency of the AFM tip motion is many times lower than the frequency of the atoms of the surface. At each step, the apex atom of the tip and atoms in the slab (except atoms on the bottom layer and H atoms which are kept fixed) are allowed to fully relax to their equilibrium positions for that particular tip position. The optimized surface structure obtained at the n th step is then used as an input (or 'seed' structure) for the $(n + 1)$th step calculations.

Atomic relaxations are performed via a conjugate gradient scheme until the energy change (ΔE) between subsequent iterations of structural optimization becomes less than 1×10^{-5} eV/atom, while the maximum forces (F_{max}) acting on the atoms are less than 1×10^{-2} eV Å^{-1}. The energy tolerance (δE) between subsequent self-consistent iterations is less than 1×10^{-6} eV/atom. It is important to notice that the convergence criteria used in the calculation to obtain an accurate reconstructed surface have to be carefully chosen. In this separated calculation for a slab we use $\Delta E = 1 \times 10^{-6}$ eV/atom, $F_{max} = 1 \times 10^{-3}$ eV Å^{-1}, and $\delta E = 1 \times 10^{-7}$ eV/atom. The BZ sampling used was a $3 \times 7 \times 1$ Monkhurst–Pack grid. Those values such as cut-off energy, k-points, etc, are chosen after extensive calculations until the final results do not depend on the choice of those values. All these convergence calculations will not be shown in the paper.

3. Results and discussion

3.1. Si(100)2 × 1 reconstructed surface

In tables 1, 2, and figure 2 we present results of the reconstructed surface. We start calculations with an initial

Table 2. z-coordinate of Si atoms for a reconstructed Si(100)2 × 1 surface obtained from our work and from LEED measurements [42]. The numbers on the left column represent the label for atoms in different layers, these numbers are also shown in figure 2.

Si atom	z-coordinate (Å)		
	LDA	GGA	LEED [42]
1	0.000	0.000	
2	0.713	0.753	0.690
3	1.331	1.393	1.430
4	1.406	1.488	1.440
5	2.620	2.726	2.630
6	2.894	2.986	3.010
7	4.022	4.138	4.080
8	4.215	4.321	4.340
9	5.488	5.590	5.570
10	5.489	5.598	5.610
11	6.865	6.967	—

unreconstructed surface structure having two dangling bonds for each atom on the surface. We provide a direct comparison of our results with experimental measurements obtained by different methods including x-ray diffraction [41], low energy electron diffraction (LEED) [42], and also AFM [16]. In addition, we compare our results with theoretical results obtained by [39, 40] and [38].

Our results show that the reconstructed Si(100)2 × 1 surface consists of asymmetric dimers with dimer bond length of 2.267 Å and a buckling angle of 18.331°, based on the LDA calculation. For the GGA calculation, these values are 2.304 Å and 18.973°, respectively. Apart from the discrepancy in the buckling angle for the GGA calculations between the present work and that of Magaud *et al* [38], our results are in excellent agreement with those of Krüger *et al* [39] and Ramstad *et al* [40]. Experimental measurements, however, for dimer bond lengths and buckling angles differ between different experimental methods, and especially for the buckling angles these vary significantly. Using grazing incidence x-ray diffraction, Jedrecy *et al* [41] have obtained a dimer bond length of 2.316 Å, with a buckling angle of 7.4°. The values obtained from LEED by Over *et al* [42] are 2.24 Å and 19.2°, respectively. Our calculations are generally in agreement with these measurements. In particular our calculations for the buckling angle obtained with GGA is in close approximation to that obtained by LEED, and the dimer bond length is in good agreement with that obtained by x-ray diffraction. Our LDA calculations are again in good approximation with LEED.
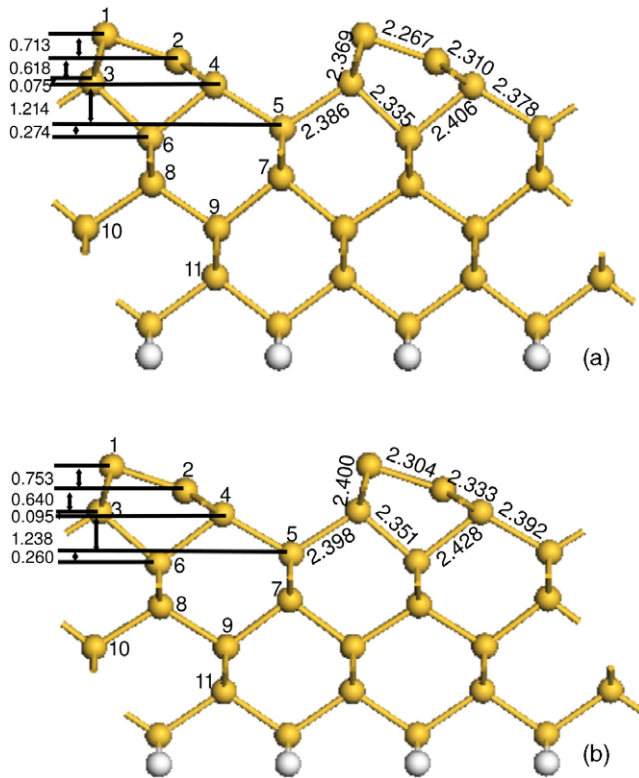
Figure 2. Bond lengths and buckling lengths for the reconstructed Si(100)2 × 1 surface obtained from LDA (a) and GGA (b) calculations.

It is interesting to note the large difference of the bond length measurement of 3.2 Å obtained with AFM in the work of Yokoyama *et al* [16] compared to those obtained by Jedrecy *et al* [41] and Over *et al* [42], and also to those obtained theoretically. However, before comparing the results obtained by AFM a further analysis and interpretation is required, taking into account the fact that in the Si(100)2 × 1 surface, dangling bonds of the two atoms in a dimer are not vertically pointing out of the surface but they tilt from the vertical direction and lie on the (101) plane which contains the dimer. Therefore the maximum interaction between the dimer atoms and the apex atom of the tip does not take place directly above the dimer atoms but at positions laterally displaced a small distance from the dimer atoms. This gives rise to the measurement error which when corrected taking this into account yields an actual dimer bond length.

The reconstructions just occur for the top layer on the surface and a few layers beneath it, other lower layers will not be affected or only affected a little under the reconstruction. Bond length of the Si dimers and the back bonds, as well as the buckling lengths for the first three layers are shown in figure 2 for both LDA and GGA calculations. The buckling lengths in this figure are shown for atoms labelled 1–6 in the first three layers and denote the buckling length between the n th and the $(n + 1)$th labelled atoms. Table 2 shows the buckling lengths for all layers for LDA and GGA methods, including data obtained by Over *et al* [42] in their LEED experiment. These are the lengths between each atom labelled 2 and 11

and the atom labelled 1. The bond lengths which correspond to the back bonds between the buckled dimer adatom and lower atom and atoms in the second layer are 2.37 Å and 2.31 Å respectively. These have been obtained by using the LDA method. The lengths obtained by the GGA method are 2.40 Å and 2.33 Å, respectively. These are in agreement with the results obtained by Ramstad *et al* [40] using LDA with norm-conserving pseudopotentials. The bond length obtained from the GGA method is larger than that from LDA. This discrepancy between LDA and GGA methods comes as no surprise, as it is known that lattice parameters (or atomic bond length) obtained from LDA are smaller by less than 0.6% than the experimental values, meanwhile values obtained from GGA are larger than experimental measurements by less than 1.5% [43]. Hence the discrepancy between LDA and GGA is less than 2.1%, which is comparable to the discrepancy in our calculations of 1.12%. For the formation of the dimer on the surface, the topmost Si atoms are asymmetrically displaced along the [101] direction. Displacements of the two topmost atoms are $\Delta x_1 = +0.483$ Å, $\Delta z_1 = +0.099$ Å and $\Delta x_2 = +1.104$ Å, $\Delta z_2 = -0.614$ Å. This results in a buckled dimer with a buckling distance of 0.713 Å. In the second layer the buckling is about 0.1 Å, this small buckling is due to the dimerization of the first layer. In the third layer the buckling is about 0.3 Å, this causes the fourth layer to buckle about 0.2 Å. For the fifth to seventh layers we do not observe any buckling as atoms in these lower layers remain at their bulk positions.

A symmetric dimer structure has also been obtained during our calculations. However, this structure is short-lived. The reason is that the total energy per dimer in this structure is higher than that of the asymmetric dimer structure with an energy difference of 0.122 eV and 0.170 eV for LDA and GGA methods, respectively. Hence the symmetric structure represents an excited state of the Si(100)2 × 1 surface but only slightly above the equilibrium ground state obtained in our calculations. However, this difference in energy per dimer between these structures is very small, and under external influences, for example with the presence of a tip or at higher temperatures, transition from asymmetric to symmetric structure can easily occur. Indeed, scans with a scanning tunnelling microscope (STM) at room temperature have obtained images of both symmetric and asymmetric dimers [44, 45]. In these experiments symmetric dimers have been observed because of thermally induced flipping of the asymmetric dimers to an excited state. As the temperature decreases, the Si dimers assume asymmetric positions again and therefore a more stable structure at lower temperatures [46]. Recently, Ono *et al* [47] have observed asymmetric dimers forming locally a c(4 × 2) structure for Si(001)2 × 1 at a temperature of 10 K, and under the influence of a tip symmetric dimers are also observed. The same observation was made by Mitsui *et al* [48] at a temperature of 65 K.

3.2. Vertical tip displacements

In this section we present results of our investigation of the short-range interaction forces between the tip and the surface
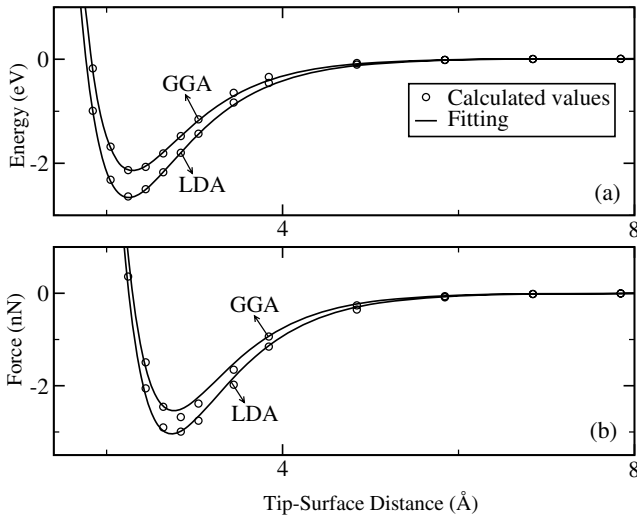
Figure 3. Total energy (a) and normal force (b) as a function of tip–surface distance when the tip scans perpendicular over the adatom. All atoms are kept fixed during calculations. The curves are plotted from calculated data and fitted using the Morse potential.

Figure 4. Total energy (a) and normal force (b) as a function of tip–surface distance when the tip scans perpendicularly over the adatom and lower atom. The apex atom of the tip and the first six layers of the surface are allowed to fully relax during the calculations.

at different tip heights. To show how the atomic relaxation affects these forces as well as how the structure changes, we carry out two different calculations, namely constrained and unconstrained calculations. First for constrained calculations, total energy and normal force are plotted as a function of tip–surface distance. The Morse potential is used to describe the potential between the dangling bonds of the surface atom and the apex atom of the tip (see figure 3(a)), which is known to provide a good description of covalent bonding in a diatomic molecule [27, 49]. This potential is given by

$$V(r) = D_0(1 - e^{-a(r-r_0)})^2 + V(r_0),$$

where r is the interatomic distance, r_0 is the equilibrium bond distances, and D_0, a, $V(r_0)$ are parameters that define the strength and range of the bonding interaction.

These parameters can be obtained from fitting the calculated data in figure 3. Results from this fitting are also shown in figure 3, with parameters $D_0 = 2.671$, $a = 1.421$, $r_e = 2.252$ for the LDA calculation. For the GGA calculation these values are $D_0 = 2.149$, $a = 1.475$, $r_e = 2.295$. For the unconstrained calculation, results of the tip moving stepwise vertically towards the adatom and the lower atom of the asymmetric dimer surface are shown in figure 4. In figure 4, the total energy is plotted as a function of the tip–surface distance, h, where h is defined as the distance from the apex atom to the adatom before any relaxation has taken place. This distance is shown in figure 1. The normal force in figure 4(b) is calculated as a numerical derivative of the total energy with respect to the tip–surface distance. In both LDA and GGA methods, the behaviour of total energy and normal force are almost the same. The minimum energy and a zero normal force are obtained when the tip–surface distance is around 1.9 Å and 2.0 Å, for LDA and GGA, respectively. The real tip–surface distances measured after the relaxation are 2.26 Å and 2.32 Å, respectively for LDA and GGA. The
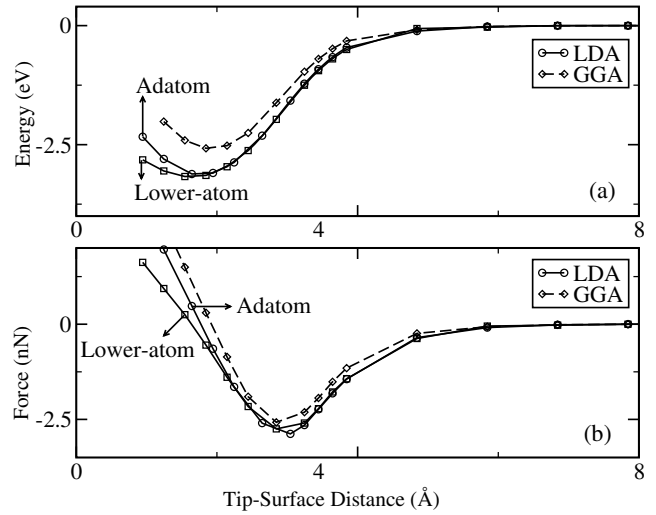
lower atom of the dimer has a buckling length of 0.713 Å with respect to the adatom as shown in figure 2. Interestingly, when the tip scans over the lower atom of the dimer at a tip–surface distance at which a minimum of the total energy exists, this point coincides with that in the case when the tip scans over the adatom. This is because the dimer flips when the tip scans sufficiently close to the lower atom. When this phenomenon occurs, the lower atom becomes the adatom and the adatom is thus pushed downwards becoming the new lower atom. This flipping starts to take place at a tip–surface distance of about 4 Å.

As we mentioned earlier, the short-range interaction between the tip and the surface is dominated by covalent chemical bonding and the force gradient is primarily responsible for the resolution in AFM imaging. We can now confirm this by comparing the force gradients for both chemical and VdW interactions. The contribution of the VdW interaction to the normal force of the tip–surface is described by the Hamaker summation method [50]. In figure 5 we show the force gradients for the tip–surface when the tip scans over the adatom and the force gradients associated with the VdW interaction assuming a spherical macroscopic tip having a measured radius of curvature of 40 Å. Results from both constrained and unconstrained calculations are shown in this figure. In constrained calculations atomic positions are kept fixed so the tip–surface distance is the real distance from the tip to the surface. Hence we can then fit the calculated data to the Morse potential as shown in figure 3 and subsequently the normal force and force gradients can be obtained by the analytical derivative of energy with respect to the distance. However, in the unconstrained calculation, atomic positions are allowed to fully relax. This results in the tip–surface distance, as defined above, not being the same as the real distance from the tip to the surface, especially in the case of short-range interactions. For this case we thus cannot fit the calculations
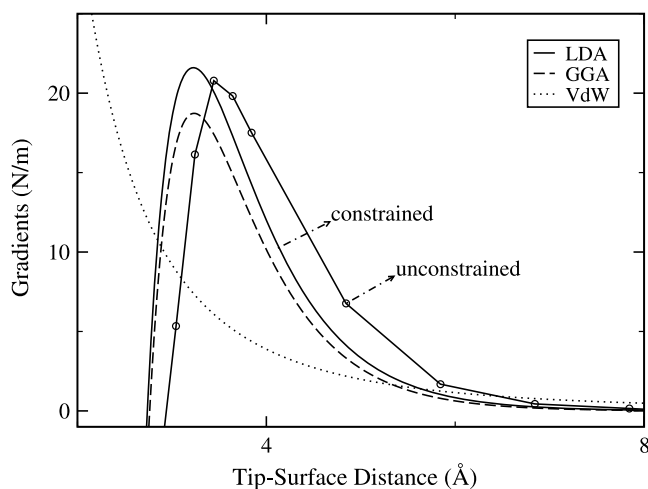
Figure 5. Force gradients for short-range interaction for both constrained and unconstrained calculations, and long-range VdW interaction for a tip of radius 40 Å.

Figure 6. (a) Total energy as a function of tip position over a scanned direction for different tip–surface distances. For tip–surface distance (h) about 4.3 Å or more, the behaviour of the energy curve is almost the same for the tip scans starting from A → B or B → A, so we just show the case with the tip scans from A → B. For tip–surface distance $h = 4$ Å we show energy curves for both directions of the scan, starting from A → B (O), and from B → A (□). (Positions A and B are also shown in figure 7.) (b) The same as (a) but this is for the normal force. Different dimer orientations when the tip scans from A → B and B → A are also shown. The new dimer after the flipping has occured is shown in a darker colour; a small dashed circle represents the new position of the adatom when the tip scans above it.

show in figure 4 to the Morse potential. Therefore, in this case, to obtain the force gradient we need to calculate the numerical derivative of the normal force with respect to the tip–surface distance h. In figure 5 we clearly see that in short-range interactions at about 2.5–5 Å the force gradient is dominated by covalent chemical interactions and when the tip is in this region adatoms are clearly obtained, implying enhanced resolution of the image. The result is almost the same from LDA and GGA calculations.

3.3. Lateral tip displacements

It has been shown that in lateral scans the variations of the force and the energy generally exhibit the same trend [27, 28, 51] and this calculated energy or force distribution can qualitatively reflect the AFM image in the frequency shift mode. In figure 6 we show the total energy and the normal force as a function of tip positions over a scanned dimer direction. Our results are shown for two different scanning directions, i.e. scanning from the adatom towards the lower atom (A → B) and vice versa, that is from the lower atom towards the adatom (B → A). Results for different tip heights over the surface are shown. The dimer orientations corresponding to positions of the tip when the tip scans from A → B and B → A are also shown in figure 6(b). The results show a fascinating behaviour of atoms on the surface induced by the tip.

Let us first analyse the case when the tip is at a height of 4 Å scanning from the adatom towards the lower atom (or from A → B). When the tip is above region A, nothing happens, this is because at this position of the tip, the distance from the tip to atoms on the surface is too high to make any interaction between them happen. However, when the tip is in the region above the adatom's dangling bond, the strong interaction between the dangling bonds of the apex atom and the adatom causes the adatom to move up and towards the apex atom. This adatom movement is shown by a small dashed circle inserted in figure 6(b) (second from left on the bottom row). This strong interaction results in a maximum in the
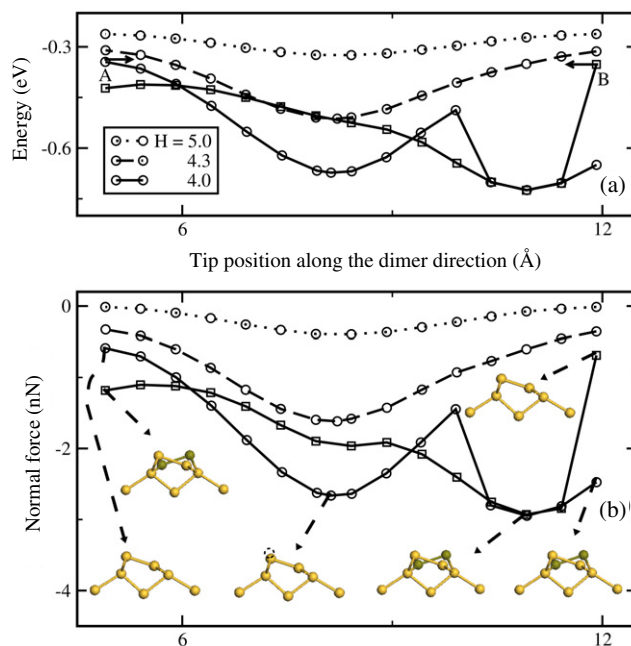
normal force, hence this adatom is clearly imaged. If we continue to move the tip to a point above the lower atom, we observe that the atoms of the dimer flip. Because of tip–surface interaction, the lower atom moves upwards and becomes the new adatom of the dimer while the original adatom moves downwards and becomes the new lower atom. Side views of the surface structures evolving when the tip moves from A → B are shown in figure 7(a). Locally, this new dimer together with the next dimers in the same row form a p(2 × 2) structure. The dimer flipping results in a lowering of the total energy or an increase in the normal force, as can be seen from the minimum energies before and after flipping takes place shown in figure 6. It lowers the energy by 0.05 eV/dimer and of course this new adatom is clearly imaged. However, when the tip moves in the opposite direction, i.e. from B → A, we observe only one atom—the new adatom after the flip when the tip was above the lower atom. As in the former case, after the flip, locally we obtain a p(2×2) structure or a c(4×2) structure. The c(4 × 2) structure is formed by a new flip dimer and an unscanned dimer ahead of it. This structure does not change during the tip moving towards A. A new dimer flip will happen when the tip moves away from A and comes close to the next lower atom. Side views of scanning along this direction are shown in figure 7(b). The comparison of the results from
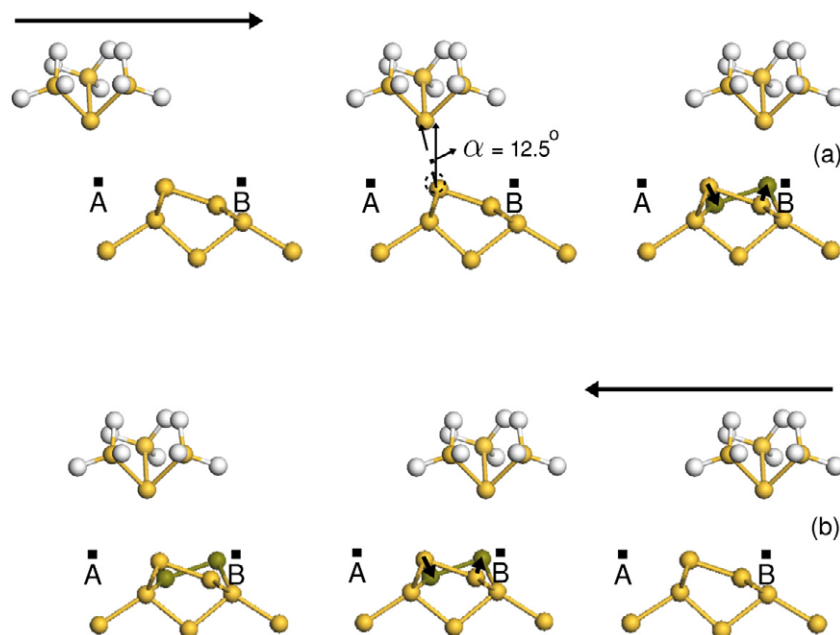
Figure 7. Side view of the structures obtained when the tip scans across the surface at $h = 4$ Å for two different scan directions. (a) Tip scans from A $\rightarrow$ B, in this case we observe both atoms of the dimer, the first one is the adatom denoted by a small dashed circle after it has moved up towards the apex atom of the tip when it is in the region of the adatom's dangling bond (the angle between the adatom's dangling bond and the vertical direction, $\alpha = 12.5°$, is shown), and the second one is the new adatom after flipping takes place (marked by arrows). (b) Tip scans from B $\rightarrow$ A, in this case we observe only one atom, it is the new adatom after flipping has taken place. When this happens the structure does not alter during the tip displacement towards A.

these two scans in figures 6 and 7 shows that the direction of scanning plays an important role in the imaging of atoms on the surface. If scanning from the adatom towards the lower atom we observe both atoms of the dimer. However, if scanning in the opposite direction only one atom can be observed.

When increasing the tip height at 4.3 Å or higher the direction of scanning plays no role in imaging as both these scans give the same result. Since at this height only the adatom can interact with the apex atom, so only this adatom can be imaged. At this height of the tip's apex atom with respect to the adatom of the surface dimer but directly above the lower atom of the dimer, the distance between the tip and the lower atom is about 5.1 Å and therefore too high. Hence interaction between them is too weak to induce any flipping. With the tip height at 5 Å, even when the tip crosses over the adatom the interaction is very weak and hence in this case no atom on the surface can be clearly observed.

Figure 6 shows that in the attractive regime the tip–surface distance plays an important role in the changes in energy and normal force, which correlates to the atomic resolution and image contrast. The normal force decreases as the tip–surface distance increases. It is important to notice that when the tip scans from A to B the two minimum points in the energy curve (or maximum in the normal force curve) are not obtained when the tip is vertically above the adatom but when it is slightly shifted away from these positions at about 0.142 Å, as shown in figures 6 and 7. This shift is due to the orientation of the adatom's dangling bond on the surface, which is tilted at an angle of 12.5° from the vertical. After subtracting these displacement shifts we obtain the real distance between these two adatoms which is about 2.5 Å.

Our results for the observation of one or two atoms per dimer have also been observed in the AFM experiment by Uchihashi *et al* [15]. Results from STM experiments at room temperature [44, 45] and at lower temperatures [47] confirmed these two structures as well.

4. Conclusions

By using density functional theory we have systematically investigated the Si(100)2 × 1 surface and the interactions between this surface and an Si tip. The buckled dimer surfaces obtained in our calculations are in very good agreement with other simulation and experimental works. We have also shown, when the tips scan over the surface, how covalent chemical interactions between the dangling bonds of the apex atom of the tip and the surface adatoms introduce dominant forces which are responsible for atomic resolution and image contrast when imaging by AFM. Calculations with full atomic relaxations in our simulations show an enhancement in atomic resolution. Furthermore, in lateral scans we have shown how the direction of scanning plays an important role in observing atoms on the surface. When the tip is at a distance of 4 Å or less above the surface and scanning from the surface dimer's adatom towards the lower atom of the dimer we can observe both atoms. However, when scanning in the opposite direction only one atom per dimer can be obtained. At distances well above 4 Å image resolution drops significantly with either the adatom or no atom at all obtained. At distances at around 4 Å, an interesting phenomenon has also been observed. At such distances we observed the surface dimer flipping with the

adatom becoming the lower atom and vice versa, leading to a localized phase transition from Si(100)2×1 to Si(100)-p(2×2).

Acknowledgments

References

[1] Binnig G, Quate C F and Gerber Ch 1986 *Phys. Rev. Lett.* **56** 930
[2] Giessibl F J 1995 *Science* **267** 68
[3] Kitamura S and Iwatsuki M 1995 *Japan. J. Appl. Phys.* **34** L145
[4] Ueyama H, Ohta M, Sugawara Y and Morita S 1995 *Japan. J. Appl. Phys.* **34** L1086
[5] Giessibl F J 2003 *Rev. Mod. Phys.* **75** 949
[6] Sugawara Y, Ueyama H, Uchihashi T, Ohta M, Morita S, Suzuki M and Mishima S 1997 *Appl. Surf. Sci.* **113/114** 364
[7] Uchihashi T, Sugawara Y, Tsukamoto T, Ohta M, Morita S and Suzuki M 1997 *Phys. Rev.* B **56** 9834
[8] Oyabu N, Custance O, Yi I, Sugawara Y and Morita S 2003 *Phys. Rev. Lett.* **90** 176102
[9] Oyabu N, Sugimoto Y, Abe M, Custance O and Morita S 2005 *Nanotechnology* **16** S112
[10] Morita S, Wiesendanger R and Meyer E 2002 *Noncontact Atomic Force Microscopy* (Berlin: Springer)
[11] Morita S, Sugimoto Y, Oyabu N, Nishi R, Custance O, Sugawara Y and Abe M 2004 *J. Electron Microsc.* **53** 163
[12] Sugimoto Y, Abe M, Hirayama S, Oyabu N, Custance O and Morita S 2005 *Nature* **4** 156
[13] Sugimoto Y, Lou P, Abe M, Jelinek P, Perez R, Morita S and Custance O 2007 *Nature* **446** 64
[14] Sugimoto Y, Pou P, Custance O, Jelinek P, Abe M, Perez R and Morita S 2008 *Science* **322** 413
[15] Uchihashi T, Sugawara Y, Tsukamoto T, Minobe T, Orisaka S, Okada T and Morita S 1999 *Appl. Surf. Sci.* **140** 304
[16] Yokoyama K, Ochi T, Yoshimoto A, Sugawara Y and Morita S 2000 *Japan. J. Appl. Phys.* **39** L113
[17] Özer H O, Atabak M and Oral A 2002 *Solid State Commun.* **124** 469
[18] Sugawara Y, Ohta M, Ueyama H and Morita S 1995 *Science* **270** 1646
[19] Allers W, Shwarz A and Wiesendanger R 1998 *Rev. Sci. Instrum.* **69** 221
[20] Orisaka S, Minobe T, Uchihashi T, Sugawara Y and Morita S 1999 *Appl. Surf. Sci.* **140** 243
[21] Loppacher Ch, Bammerlin M, Guggisberg M, Schär S, Bennewitz R, Baratoff A, Meyer E and Güntherodt H-J 2000 *Phys. Rev.* B **62** 16944
[22] Bammerlin M, Lüthi R, Meyer E, Baratoff A, Lü J, Guggisberg M, Gerber Ch, Howald L and Güntherodt H-J 1997 *Probe Microsc.* **1** 3
[23] Barth C and Reichling M 2001 *Nature* **414** 54
[24] Nishi R, Miyagawa D, Seino Y, Yi I and Morita S 2006 *Nanotechnology* **17** S142
[25] Garcia R and Perez R 2002 *Surf. Sci. Rep.* **47** 197
[26] Perez R, Payne M, Stich I and Terakura K 1997 *Phys. Rev. Lett.* **78** 678
[27] Perez R, Stich I, Payne M C and Terakura K 1998 *Phys. Rev.* B **58** 10835
[28] Ke S H, Uda T, Perez R, Stich I and Terakura K 1999 *Phys. Rev.* B **60** 11631
[29] Perez R, Stich I, Payne M C and Terakura K 1999 *Appl. Surf. Sci.* **140** 320
[30] Foster A S, Kantorovich L N and Shluger A L 2001 *Appl. Phys.* A **72** S59
[31] Dabrowski J and Müssig H J 2000 *Silicon Surfaces and Formation of Interfaces* (Singapore: World Scientific)
[32] Keeling D L, Humphry M J, Moriarty P and Beton P H 2002 *Chem. Phys. Lett.* **366** 300
[33] Moriaty P, Ma Y R, Upward M D and Beton P H 1998 *Surf. Sci.* **407** 27
[34] Payne M C, Teter M P, Allan D C, Arias T A and Joannopoulos J D 1992 *Rev. Mod. Phys.* **64** 1045
[35] Clark S J, Segall M D, Pickard C J, Hasnip P J, Probert M J, Refson K and Payne M C 2005 *Z. Kristallogr.* **220** 567
[36] Perdew J P and Zunger A 1981 *Phys. Rev.* B **23** 5048
[37] Perdew J P, Burke K and Ernzerhof M 1996 *Phys. Rev. Lett.* **77** 3865
[38] Magaud L, Pasturel A, Jure L, Mallet P and Veuillen J Y 2000 *Surf. Sci.* **454** 489
[39] Krüger P and Pollmann J 1994 *Appl. Phys.* A **59** 487
[40] Ramstad A, Brocks G and Kelly P J 1995 *Phys. Rev.* B **51** 14504
[41] Jedrecy N, Sauvage-Simkin M, Pinchaux R, Massies J, Greiser N and Etgens V H 1990 *Surf. Sci.* **230** 197
[42] Over H, Wasserfall J, Ranke W, Ambiatello C, Sawitzki R, Wolf D and Moritz W 1997 *Phys. Rev.* B **55** 4731
[43] Filippi C, Singh D J and Umrigar C J 1994 *Phys. Rev.* B **50** 14947
[44] Tromp R M, Hamers R J and Demuth J E 1985 *Phys. Rev. Lett.* **55** 1303
[45] Hamers R J, Tromp R M and Demuth J E 1986 *Phys. Rev.* B **34** 5343
[46] Wolkow R A 1992 *Phys. Rev. Lett.* **68** 2636
[47] Ono M, Kamoshida A, Matsuura N, Ishikawa E, Eguchi T and Hasegawa Y 2003 *Phys. Rev.* B **67** 201306
[48] Mitsui T and Takayanagi K 2000 *Phys. Rev.* B **62** R16251
[49] Olsson L, Wigren R and Erlandsson R 1996 *Rev. Sci. Instrum.* **67** 2289
[50] Israelachvili J 1992 *Intermolecular and Surface Forces* (London: Academic) p 176
[51] Ke S H, Uda T and Terakura K 1999 *Phys. Rev.* B **59** 13267